

# A new fast reconnection model in a collisionless regime

David Tsiklauri

*Joule Physics Laboratory, Institute for Materials Research,  
University of Salford, Manchester, M5 4WT, United Kingdom*

(Dated: November 2, 2018)

Based on the first principles (i.e. (i) by balancing the magnetic field advection with the term containing electron pressure tensor non-gyrotropic components in the generalised Ohm's law; (ii) using the conservation of mass; and (iii) assuming that the weak magnetic field region width, where electron meandering motion supports electron pressure tensor off-diagonal (non-gyrotropic) components, is of the order of electron Larmor radius;) a simple model of magnetic reconnection in a collisionless regime is formulated. The model is general, resembling its collisional Sweet-Parker analogue in that it is not specific to any initial configuration e.g. Harris type tearing unstable current sheet, X-point collapse or otherwise. In addition to its importance from the fundamental point of view, the collisionless reconnection model offers a much faster reconnection rate ( $M_{c'less} = (c/\omega_{pe})^2/(r_{L,e}L)$ ) than Sweet-Parker's classical one ( $M_{sp} = S^{-1/2}$ ). The width of the diffusion region (current sheet) in the collisionless regime is found to be  $\delta_{c'less} = (c/\omega_{pe})^2/r_{L,e}$ , which is independent of global reconnection scale  $L$  and is only prescribed by micro-physics (electron inertial length,  $c/\omega_{pe}$ , and electron Larmor radius,  $r_{L,e}$ ). Amongst other issues, the fastness of the reconnection rate alleviates e.g. the problem of interpretation of solar flares by means of reconnection, as for the typical solar coronal parameters the obtained collisionless reconnection time can be a few minutes, as opposed to Sweet-Parker's equivalent value of  $< 1$  day. The new theoretical reconnection rate is compared to the MRX (Magnetic Reconnection Experiment) device experimental data by Yamada et al. [1], Ji et al. [2] and a good agreement is obtained.

PACS numbers: 52.35.Vd; 96.60.Iv; 52.65.Rr; 45.50.Dd; 96.60.pf; 96.60.qe

## I. MOTIVATION

Magnetic reconnection is the process that enables to convert magnetic energy into heat and kinetic energy of accelerated particles [3, 4, 5]. In many astrophysical and laboratory plasma situations plasma beta (the ratio of thermal and magnetic pressures) is much smaller than unity. Thus, magnetic reconnection has attracted a considerable attention as the plasma heating and charged particle acceleration mechanism. It is believed that magnetic reconnection is responsible for solar [6, 7] and stellar flares [8, 9]. It has been also observed in the Earth geomagnetic tail [10].

This work has several motivations:

(i) The longstanding problems with resistive MHD (Magnetohydrodynamic), i.e. *collisional* description of the magnetic reconnection has been its too slow rate if a consistent, the-first-principles approach is used [11, 12]; or a fast rate [13], but a lack of a proper motivation ([4], p. 79) (one can still get the fast reconnection if the resistivity is enhanced in the diffusion region, as one expects in physical applications). In the *collisionless* regime there is no known simple, analytical reconnection rate (e.g. analogous to Sweet-Parker, or Petschek rates). What does exist, however, is a bulk of mostly numerical simulation work [14, 15, 16, 17, 18]. It should be mentioned that a significant progress (including analytical) has been made in study of the details of collisionless reconnection such as the diffusion region structure, outflows, reconnection rates [14, 19, 20, 21]. However these were either specific to a narrow class of collisionless reconnection models, namely tearing unstable Harris current sheet; or too

slow reconnection rates were obtained [22]. Some numerical simulation models [14, 15, 16, 17, 18, 19, 20, 21] can produce as fast reconnection rates as  $M > 0.5$  where  $M$  is the inflow Alfvénic Mach number. The lack of a simple, analytical model of collisionless reconnection (*that is not specific to any initial configuration*) has been somewhat hampering the progress in understanding.

(ii) Quite often, particularly in space plasmas, there is a good reason to go beyond resistive, single-fluid MHD. A simple line of reasoning can be outlined on an example of e.g. solar corona. Fixing coronal temperature at  $1.0 \times 10^6$  K, Coulomb logarithm at 18.1, the Lundquist number (using Spitzer resistivity) is  $3.7 \times 10^{11}$ . Here  $L = 10^5$  m was used. One of the arguments for going beyond resistive MHD is comparing typical width of a Sweet-Parker current sheet  $\delta_{sp} = S^{-1/2}L = 0.16$  m to the ion inertial length. Typical scale associated with the Hall term in the generalised Ohm's law at which deviation from electron-ion coupled dynamics is observed is,  $c/\omega_{pi} = 7.2$  m. Here particle density of  $n = 1.0 \times 10^{15}$  m $^{-3}$  is used. Hence, the fact that  $c/(\omega_{pi}\delta_{sp}) = 44 \gg 1$  warrants going *beyond single fluid resistive MHD approximation* (a similar conclusion is reached by Yamada et al. [1] in their Figure 12 based on laboratory plasma experiment known as MRX (Magnetic Reconnection Experiment)).

(iii) Previous results on collisionless reconnection both in tearing unstable Harris current sheet [14, 15, 16, 19] and stressed X-point collapse [17, 18] has shown that magnetic field is frozen into electron fluid and the term in the generalised Ohm's law that is responsible for breaking the frozen-in condition is electron pressure tensor off-diagonal (non-gyrotropic) components. Thus, a need for

inclusion of the *electron pressure tensor non-gyrotropic components* in a model of collisionless reconnection has become clear.

(iv) There is a growing amount of work [5, 17, 18] that suggests that in the collisionless regime, on the scales less than  $c/\omega_{pi}$  magnetic field is frozen into the electron fluid rather than bulk of plasma. One can write in general  $\vec{V}_e = \vec{V}_i - \vec{j}/(en)$ . This relation clearly shows that in collisional regime (when the number density  $n$  is large), the difference between electron and ions speeds diminishes  $V_e = V_i = V$ . However, as one enters collisionless regime (when the number density  $n$  is small) the deviation between electron and ion speeds starts to show. In Tsiklauri and Haruki [18] we proposed a possible explanation why the reconnection is fast when the Hall term is included. Inclusion of the latter means that in the reconnection inflow magnetic field is frozen into *electron* fluid. As it was previously shown in Tsiklauri and Haruki [17] (see their Figs.(7) and (11)) speed of electrons, during the reconnection peak time, is at least 4-5 times greater than that of ions. This means that electrons can bring in / take out the magnetic field attached to them into / away from the diffusion region much faster than in the case of single fluid MHD which does not distinguish between electron-ion dynamics. Thus, a need for inclusion *magnetic field transport by electrons* in a model of collisionless reconnection has become clear.

(v) A pioneering work of Yamada et al. [1] has demonstrated a clear transition from collisional to collisionless reconnection regimes by varying the plasma density, and established that in the collisionless regime the reconnection rate is much greater than the Sweet-Parker rate. Despite a well motivated explanation of their experimental results, one was surprised to see only experimental data points and numerical simulation results on their Figure 12. Thus, we set out with a task of formulating a simple model of magnetic reconnection in a collisionless regime. In what follows we shall be using well-motivated arguments of Sweet-Parker model, but shall be applying it to the collisionless case.

## II. THE MODEL

It is instructive to re-iterate key points of the Sweet-Parker model. The first step towards the derivation of the reconnection rate is that the plasma outflow speed from the diffusion region is of the order of the Alfvén speed,  $V_{outflow} = V_A = B_0/\sqrt{\mu_0 m_i n} = B_0/\sqrt{\mu_0 \rho}$ . This follows from the following consideration: taking the fluid to be incompressible and assuming a steady state condition, one obtains [23], p. 285

$$\frac{\rho V_{outflow}^2}{2} = p_i - p_o, \quad (1)$$

where  $p_i$  and  $p_o$  are thermal pressures inside and outside the diffusion region. This pressure difference can be set to

the magnetic pressure  $B_0^2/(2\mu_0)$ . From which the above result  $V_{outflow} = V_A$  readily follows.

The second step is applying the continuity equation

$$V_{inflow}L = V_A\delta, \quad (2)$$

where  $L$  and  $\delta$  are the diffusion region length and width respectively.

The third step is using the generalised Ohm's law (e.g. [5] p. 108)

$$\vec{E} = -\vec{v}_e \times \vec{B} - \frac{\nabla \cdot \vec{P}_e}{n_e e} - \frac{m_e}{e} \left( \frac{\partial \vec{v}_e}{\partial t} + (\vec{v}_e \cdot \nabla) \vec{v}_e \right) + \eta \vec{j}, \quad (3)$$

where  $\vec{E}$  and  $\vec{B}$  are electric and magnetic fields,  $\vec{v}$  is plasma velocity,  $\vec{P}$  is pressure tensor ( $3 \times 3$  matrix),  $n$  is plasma number density,  $m$  is mass and  $e$  is electric charge. Subscript  $e$  stands for an electron. In Eq.(3) we balance two terms advection ( $\vec{v}_e \times \vec{B}$ ) and resistive diffusion ( $\eta \vec{j}$ ):

$$V_{inflow}B_0 = \eta j = \eta B_0/(\mu_0 \delta), \quad (4)$$

where  $\vec{j} = (\nabla \times \vec{B})/\mu_0$  is used, with  $\nabla \approx 1/\delta$ . Note that in the (collisional) resistive MHD regime all other terms in the generalised Ohm's law are insignificant and  $V_e = V_i = V$ . Finally, substituting  $(1/\delta)$  from Eq.(2) and after some simple algebra one arrives at

$$M_{sp} \equiv V_{inflow}/V_A = S^{-1/2}, \quad (5)$$

Where  $S = \mu_0 L V_A / \eta$ , the Lundquist number has been introduced. Eq.(5) constitutes the classical Sweet-Parker reconnection rate.

In order to obtain collisionless reconnection rate in an analogy with the above derivation of the classical Sweet-Parker rate, we now balance the advection ( $\vec{v}_e \times \vec{B}$ ) with electron pressure tensor ( $\nabla \cdot \vec{P}_e / (n_e e)$ ), because now Spitzer resistivity in the collisionless regime is not large enough and also  $V_e \neq V_i = V$ . Previous results of the reconnection in the collisionless regime, both in tearing unstable Harris current sheet [14, 15, 16] and stressed X-point collapse [17, 18], have shown that: (i) the term in the generalised Ohm's law that is responsible for breaking the frozen-in condition is electron pressure tensor non-gyrotropic components and (ii) the magnetic field is frozen into electron fluid. Kuznetsova et al. [19] formulate two dimensional model, which shows that in a steady state, at the magnetic null (X-point) where the electron flow velocities and magnetic field are zero, the only terms in the generalized Ohm's law that can support out-of-plane electric field (and hence the reconnection) are electron pressure tensor non-gyrotropic components (see their Eqs.(4)-(6)):

$$E_y^{NG} = -\frac{1}{ne} \left( \frac{\partial P_{xy}}{\partial x} + \frac{\partial P_{zy}}{\partial z} \right). \quad (6)$$

Here the two  $x$ - and  $z$ -coordinates are along (outflows) and across (inflows) the current sheet respectively. Further simplification can be made observing that  $P_{xy} \approx P_{zy}$

but  $\partial/\partial z \gg \partial/\partial x$  because width of the current sheet is much smaller than its length:

$$E_y^{NG} \approx -\frac{1}{ne} \frac{P_{zy}}{\delta_{c'less}}, \quad (7)$$

where  $\delta_{c'less}$  is the width of the current sheet in the collisionless regime ( $\partial/\partial z \approx \delta_{c'less}$ ). Thus in an analogy with Eq.(4) we now have

$$E_y^{NG} = V_{e,inflow} B_0 \approx -\frac{1}{ne} \frac{P_{zy}}{\delta_{c'less}}. \quad (8)$$

Note that the latter equation is similar to Eq.(11) from Hesse et al. [14]. In addition to balancing the different terms, note also that the two crucial differences from Eq.(4) are that (i) we use electron speed  $V_{e,inflow}$  because magnetic field advection on scales less than  $c/\omega_{pi}$  is done by electrons and (ii) width of the diffusion region (current sheet) is  $\delta_{c'less}$  which we shall specify below.

Let us now specify electron pressure tensor non-gyrotropic component  $P_{zy}$ . Based in earlier works, which use second moment of Vlasov equation (i.e. multiplying the Vlasov equation by  $v_i v_j$  and integrating over the velocity space), Kuznetsova et al. [19] give explicit expression for the electron pressure tensor components. Intermediate expression for  $P_{zy}$  in the static case, which is generic and yet is not specific to tearing unstable Harris current sheet configuration, is given by Eq.(14) in Kuznetsova et al. [19]:

$$P_{zy} = -\frac{P_{zz}}{2\Omega_x} \frac{\partial v_{ez}}{\partial z}, \quad (9)$$

where  $\Omega_x = (eB_0/m_e)(z/\delta_{c'less})$  takes into account linear variation of magnetic field with distance in the vicinity of the magnetic null. The electron pressure tensor non-gyrotropic (off-diagonal) components are generally much smaller than gyrotropic (diagonal) ones. The deviations from gyrotropic pressure are possible due to electron meandering motion in the regions of weak magnetic field close to the x-point [24]. Away from the x-point the particles are magnetized and pressure is isotropic. Thus, it would be reasonable to assume that electron meandering motion will be effective up to  $z \approx r_{L,e}$ . Here  $r_{L,e} = v_{th,e}/\omega_{ce}$  is the electron Larmor radius.  $v_{th,e} = \sqrt{k_B T/m_e}$  is electron thermal speed and  $\omega_{ce} = eB/m_e$  is electron cyclotron frequency. Further away from the magnetic null, when  $z \gg r_{L,e}$  then pressure becomes isotropic. Thus in the above expression for  $\Omega_x$  we set  $z \approx r_{L,e}$ , i.e.  $\Omega_x = (eB/m_e)(r_{L,e}/\delta_{c'less})$ . In Eq.(9) we can also assume the gyrotropic pressure component  $P_{zz}$  is of the order of the magnetic pressure  $B_0^2/(2\mu_0)$ , set  $v_{ez}$  as the electron inflow speed  $V_{e,inflow}$ , also estimate  $\partial/\partial z \approx 1/\delta_{c'less}$ . Thus for the  $P_{zy}$  we have

$$P_{zy} = -\frac{B_0^2}{2\mu_0} \frac{m_e}{eB_0} \frac{\delta_{c'less}}{r_{L,e}} \frac{V_{e,inflow}}{\delta_{c'less}}. \quad (10)$$

Naturally, the next step is to specify width of the diffusion region in the collisionless regime, which we do by

using conservation of mass, but again taking into account that now magnetic field is advected by the electrons. Thus, in lieu of Eq.(2) we have

$$V_{e,inflow} L = V_{e,A} \delta_{c'less}, \quad (11)$$

where  $V_{e,A} = B_0/\sqrt{\mu_0 n m_e} = V_A \sqrt{m_i/m_e}$  is the *electron* Alfvén speed.

Thus substituting Eq.(10) into Eq.(8), using Eq.(11) and defining the collisionless inflow Alfvénic Mach number,  $M_{c'less}$  as  $M_{c'less} = V_{e,inflow}/V_{e,A}$ , after simple algebra (also noting that  $ne^2/m_e = \omega_{pe}^2/\epsilon_0$  and  $c = 1/\sqrt{\mu_0 \epsilon_0}$ ) we obtain

$$M_{c'less} \equiv \left( \frac{c}{\omega_{pe}} \right)^2 \frac{1}{r_{L,e} L}. \quad (12)$$

Note that factor 1/2 has been omitted because this rate is a crude estimate.

Eq.(12) can be regarded as the main result of this work, as it provides the collisionless reconnection rate independent of an initial configuration.

Simple analysis shows that collisionless reconnection rate  $M_{c'less} = 1.3 \times 10^{-4}$  e.g. for solar coronal parameters ( $n = 1.0 \times 10^{15} \text{ m}^{-3}$ ,  $T = 1.0 \times 10^6 \text{ K}$ ,  $L = 10^5 \text{ m}$ ,  $B = 0.01 \text{ T}$  (100 Gauss and hence  $V_A = 6.9 \times 10^6 \text{ m s}^{-1}$ ),  $S = 3.7 \times 10^{11}$ ) is two orders of magnitude faster than the classical Sweet-Parker rate  $M_{sp} = 1.6 \times 10^{-6}$ . In the context of solar flares this means that the collisionless model, presented here, effectively alleviates longstanding problem of the interpretation of solar flares by means of magnetic reconnection. The reconnection rate is also interpreted as the ratio of Alfvén time ( $\tau_A = L/V_A \approx 0.0145 \text{ s}$ ) and resistive (or reconnection) times. This means in the Sweet-Parker model resistive (or reconnection) time is  $0.0145/S^{-1/2} \text{ s} = 0.1 \text{ days}$ . While our model provides reconnection time of  $0.0145/(1.3 \times 10^{-4}) \text{ s} = 2 \text{ minutes}$ , which is commensurate of solar flare observations. It should be mentioned that Petschek model also can provide an appropriately fast reconnection rate, although its justification from the fundamental point of view is not without a debate [4].

We now shall compare the master equation Eq.(12) to the MRX experimental data of Yamada et al. [1]. Their figure 12 presents how the empirical reconnection rate scales with the parameter  $c/(\omega_{pi} \delta_{sp})$ , which is essentially the ratio of ion inertial length and the width of the Sweet-Parker current sheet. Yamada et al. [1] have clearly established that in the collisionless regime, i.e. when  $c/(\omega_{pi} \delta_{sp}) \gg 1$  the normalised reconnection rate (after starting from the Sweet-Parker rate) attains values much larger than unity. In order to compare our scaling law, Eq.(12) to the data from Ref.[1], we need to normalise the collisionless reconnection rate by the Sweet-Parker rate  $S^{-1/2}$ . Also, in order for the results to be applicable in the collisional regime too, we combine collisional and collisionless rates as follows:  $M = M_{sp} + M_{c'less}$ . Noting

that  $L = \delta_{sp} S^{1/2}$  we obtain,

$$M/M_{sp} = 1 + \frac{m_e}{m_i} \frac{\delta_{sp}}{r_{L,e}} \left( \frac{c}{\omega_{pi} \delta_{sp}} \right)^2. \quad (13)$$

Note that despite a factor  $m_e/m_i$  appearing in Eq.(13),  $M/M_{sp}$  does not depend on ion mass as  $1/\omega_{pi}^2 \propto m_i$ . Also the same is evident from the fact that  $M_{c'less}$  (according to Eq.(12)) only contains physical quantities pertaining to an electron, and  $M_{sp}$  is independent of ion mass, so should be their sum. Our collisionless reconnection rate seems to fit the experimental data [1] and the two-fluid simulation results [25] well in the range  $c/(\omega_{pi} \delta_{sp}) \gg 1$ . It should be noted that each experimental data point was obtained for different plasma parameters. Hence each data point has its own  $S$  associated with it.  $S$  changes from roughly 200 to 800 as we move in the lowest measured values of  $c/(\omega_{pi} \delta_{sp}) = 1.5$  to  $c/(\omega_{pi} \delta_{sp}) = 10$  in the horizontal axis (M. Yamada, private communication). In order to provide theoretical *curves* rather than sets of the theoretical points we argue that in Eq.(13) the dependence on  $S$  is weak (via  $\propto \delta_{sp} = LS^{-1/2}$ ). Therefore, solid curve in Fig.1 is produced using a fixed value of  $S = 200$ . Other parameters used in Fig. 1 were  $T = 5$  eV,  $L = 0.4$  m and  $B = 0.05$  Tesla. Some deviation in the region of  $c/(\omega_{pi} \delta_{sp}) \approx 1$  can be explained by, perhaps, several factors that were not taken into account in our simple model. Let us mention the obvious two: (i) Strictly speaking our reconnection rate Eqs.(12) or (13) was obtained assuming a steady state, while as Yamada et al. [1] mention, the pull magnetic reconnection lasts for about 40  $\mu$ s. Although this is much longer than the typical Alfvén time  $\leq \mu$ s, yet one can argue that *nearly* steady state was achieved in the experiment. Thus the comparison between the theory and experiment should be taken with caution. (ii) Our theoretical reconnection rate, naturally, does not include contributions from turbulence. Despite these shortcomings the match between the theory and experiment seems good.

Based on Eqs.(11) and (12) it is also straightforward to derive the width of the diffusion region (current sheet) in the collisionless regime:

$$\delta_{c'less} = M_{c'less} L = \left( \frac{c}{\omega_{pe}} \right)^2 \frac{1}{r_{L,e}}, \quad (14)$$

which is independent of global reconnection scale  $L$  and is only prescribed by micro-physics (electron inertial length,  $c/\omega_{pe}$ , and electron Larmor radius,  $r_{L,e}$ ).

Ji et al. [2] have provided MRX laboratory experimental data and 2D Particle-In-Cell simulation results of scaling of the electron diffusion region width,  $\delta_e$ , with the electron inertial length,  $c/\omega_{pe}$ . It was found that the experimental data can be fitted with a straight line  $8c/\omega_{pe}$ , while PIC simulation data consistently produced a less steep scaling of  $1.6c/\omega_{pe}$ . Naturally, we tried to apply the diffusion region (current sheet) width formula from our model (Eq.(14)) to Ji et al. [2]. Useful sketch to aid visualisation can be found in Birn and Priest [5],

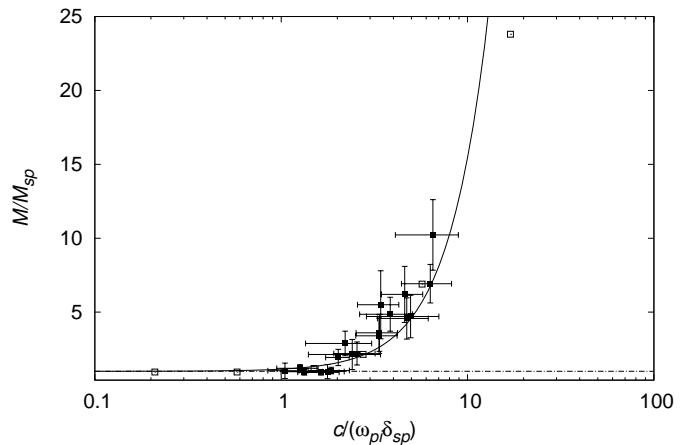


FIG. 1: Solid curve shows collisionless reconnection rate normalised to the Sweet-Parker rate according to Eq.(13) versus  $c/(\omega_{pi} \delta_{sp})$ . Note that Hydrogen, Deuterium and Helium plasmas are all represented by the same solid curve, as  $M/M_{sp}$  is independent of an ion mass. Data points with error bars correspond to MRX data Yamada et al. [1]. Note that in data we do not distinguish between the species. Open square symbols are the 2D two-fluid simulation results by Breslau and Jardin [25]. Dash-dotted line represents the Sweet-Parker rate.

p.91, Fig.3.1. When plasma inflows in the diffusion region ions decouple from electrons at ion inertial length scale of  $\approx c/\omega_{pi}$ , while electrons deflect from the diffusion region (and hence forming it) at electron inertial length scale of  $\approx c/\omega_{pe}$ . One of the convincing findings of Ji et al. [2] was that the electron diffusion region width,  $\delta_e$ , is independent of which ion species are used in the experiment (H, D<sub>2</sub> or He). Thus one can conclude that they indeed were observing electron diffusion region. This corroborates the fact that at the electron inertial length scales the magnetic field transport is done by electrons, as well as the currents are carried by electrons. Our width of the diffusion region according to Eq.(14) is shown as solid curve in Fig.2. A reasonably good fit is obtained, supporting the idea that Eq.(14) indeed provides a good theoretical expression for the electron diffusion region width.

### III. DISCUSSION

Let us estimate the coronal heating flux which is produced by our collisionless reconnection model. One can obtain the heating flux ( $\text{W m}^{-2}$ ) by taking magnetic energy density  $B^2/(2\mu_0)$  ( $\text{J m}^{-3}$ ), multiplying it by a typical scale  $L = 10^5$  m and dividing by the reconnection times which we estimated above,  $t_{c'less} = \tau_A/M_{c'less} = 114$  s (2 min) and  $t_{sp} = \tau_A/M_{sp} = 8831$  s (0.1 days) – assuming the reconnection time is a good proxy for the energy release time in the solar corona. Fixing  $B = 0.01$  T, in the case of collisionless reconnection, the heating flux is obtained  $3.5 \times 10^4 \text{ W m}^{-2}$ , which is more than

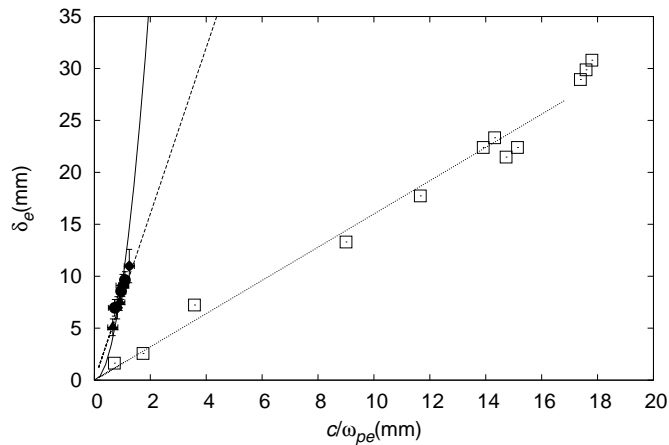


FIG. 2: Solid curve shows  $\delta_{c'less}$  according Eq.(14). Dashed and dotted lines represent  $8c/\omega_{pe}$  and  $1.6c/\omega_{pe}$  respectively. Solid symbols with error bars are MRX experimental measurements, while open squares are PIC simulation results – both from Ji et al. [2]. Here  $T = 5$  eV and  $B = 0.05$  Tesla.

enough to meet the coronal heating requirement; while as expected Sweet-Parker model produces an equivalent of  $450 \text{ W m}^{-2}$ . Aschwanden [26], p. 359 quotes solar active region typical heating requirement value of  $2000 \text{ W m}^{-2}$ . The obtained collisionless reconnection heating flux is an order of magnitude larger than that. Naturally, neither all of the collisionless reconnection heating flux will go into dissipation (by definition collisionless process is dissipationless), nor all 100% of the magnetic energy will be released by the reconnection process. Even if 1/10th of it will ultimately end up as the heat, then the coronal heating requirement can be met. Thus, the importance of the present model for the coronal heating seems evident.

Next, let us comment on the observational consequences of the collisionless reconnection model in solar coronal context. The reconnection time (the flare energy release time),  $t_{c'less} = \tau_A/M_{c'less} \propto L^2$  (because,  $\tau_A = L/V_A$ , and  $M_{c'less} \propto 1/L$ ). Thus, if we assume that magnetic field and plasma density remains the same as we go from small to large flares (this assumption implies that for simplicity of the argument  $V_A$  in  $\tau_A$  and  $c/\omega_{pe}$  in Eq.(12) stay the same), the flare time should increase (quadratically) with flare size. There is some ambiguity how to define actual spatial size of a flare (Dr. E. Kontar of University of Glasgow, private communication): At high energies one sees loop footpoints only; Hence is the geometric size a distance between the footpoints or total (unknown) area? In soft X-rays (6-10 keV) only the loop-top source is observed. X-Ray telescope (XRT) on board of Japanese space mission Hinode often sees the entire flaring loop. However, this mission is quite recent and no good flare statistics exists as yet. Temmer et al. [27] claim that the flare duration increases with increasing the flare importance class, hence with the flare area, as re-

ported by a number of papers (see their Table 7). Based on a statistical analysis of almost 50 000 soft X-ray flares observed during the period 1976-2000 Veronig et al. [28] show that the scatter plots of the flare duration, rise time and decay time as function of the flare fluence ( $\text{J m}^{-2}$ ) show strong correlations. Whether the latter is a good proxy of the flare geometrical size is not entirely certain. Nagashima and Yokoyama [29] report a statistical study of flares observed with the Soft X-Ray Telescope (SXT) on board of Yohkoh in the year 2000. They measured physical parameters of 77 flares. Their Fig. (3) plots the spatial scale  $L$  against the flare timescale and shows that the spatial scale  $L$  tends to be larger with the increasing timescale. Thus, in summary, our scaling seems to be in agreement with the solar flare observations. One should be aware of the fact that in the solar flare observations we see only post-reconnection dynamics and the geometric size of "particle accelerator", the location of actual energy deposition site is never resolved, due to poor spatial resolution of the instruments. Some source of a concern is also the aspect ratio of the diffusion region (i.e. the current layer, where particles are accelerated). From Eq.(14) it is clear for  $M_{c'less} = 1.3 \times 10^{-4}$  the aspect ratio is about 7500 : 1. The question is whether such fine scale structure can survive in the turbulent corona. However, since current observations do not have enough resolution to prove or disprove existence of such elongated current layers, the jury is still out.

On the laboratory plasma side, comparison of our model scaling with the MRX data (see Fig.(2)) needs a clarification as to why PIC simulation results (open squares) do not fit the experimental data while our simple analytical model does. At first sight one might expect the opposite to be true because PIC simulation includes all relevant physics, i.e. all relevant terms in the generalized Ohm's law, time dependence, etc. In author's opinion the source of the discrepancy are the boundary conditions and the mass ratio mismatch. Ji et al. [2] (see their Fig. 3) either use boundary conditions commensurate to MRX (conducting boundary conditions for electromagnetic fields and elastic reflection of particles at wall) for unrealistic mass ratio of 400, or open boundary conditions for a realistic mass ratio of 1836 (for Hydrogen only). It is no surprise that the outcomes of numerical simulations depend on correct (appropriate) boundary conditions used. There are two issues here: first, when MRX boundary conditions are used, it may well be that a better fit could have been achieved, if the correct mass ratio were used (note that experimental data points lie on the line ( $8c/\omega_{pe}$ ) that is factor of  $\approx 5$  above PIC simulation line  $1.6c/\omega_{pe}$ . Accidentally such is also the mass ratio mismatch  $1836./400 = 4.6$ . Note, however, that the theoretically derived width according to Eq.(14) scales as  $\propto 1/(\omega_{pe}^2 r_{L,e}) \propto m_e \times \omega_{ce}/v_{th,e} \propto m_e \times m_e^{-1} \times \sqrt{m_e} \propto \sqrt{m_e}$ ). Hence if our analytical treatment is correct, Eq.(14) still does not alleviate the problem in full, as  $\sqrt{1836./400} = 2.1$  cannot account for the factor of 5 difference between the MRX data and PIC

simulations. But the trend is in the right direction; Secondly, when the correct mass ratio is used (in Ref.[2], Fig.3) open boundary conditions are not a good representation of the experiment. Hence the results based on open boundary conditions should be discarded. Thus, we conjecture that when simultaneously (a) the correct mass ratio and (b) boundary conditions commensurate to MRX are used, than PIC simulation results will possibly follow our theoretical result (Eq.(14)). Until such simulation is performed, however, the jury in this issue is still out.

Some clarification is necessary concerning the use of notation for  $L$ . In Eq.(11) it plays a role of the *electron* diffusion region length; i.e. the region of space where the electron dynamics is decoupled from that of ions. Since in the solar flare observations the geometric size of "particle accelerator", the location of actual energy deposition site is never resolved, due to poor spatial resolution of the instruments, we use  $L = 10^5$  m, a typical length scale in the corona. In context of MRX, we use the length of the magnetic scale  $L = 0.4$  m. However, on the MHD scale (to which our numerical estimates apply) one also expects that at some distance downstream from the X-point, electron and ion dynamics becomes coupled again. This implies that the outflowing electrons will decelerate from the electron Alfvén speed to ion Alfvén seed. Recent PIC simulations [30, 31] suggest that the electron diffusion region length can extend for much longer distances downstream than previously thought, and hence alleviating, in part, the above problem.

#### IV. CONCLUSIONS

A new model of collisionless reconnection is formulated that is based on simple conservation

laws. The obtained collisionless reconnection rate,  $M_{c'less} = (c/\omega_{pe})^2/(r_{L,e}L)$ , naturally does not depend on Lundquist number,  $S$ , (because it is collisionless) and is much faster than the Sweet-Parker rate, but yet somewhat slower than the Petschek rate (at least for solar coronal plasma parameters). In particular, for the same set of parameters e.g. for solar coronal plasma the rates are  $M_{petschek} = 0.04$ ,  $M_{c'less} = 1.3 \times 10^{-4}$ ,  $M_{sp} = 1.6 \times 10^{-6}$ . The main implication for solar flares is that if this collisionless rate is used, flare time can be as short as a few minutes, that is commensurate with the observations. Note that the formulated collisionless reconnection model is general and is not specific to any initial configuration e.g. Harris type tearing unstable current sheet, X-point collapse or otherwise. In differ to previous results it relates the reconnection rate to simple, generic spatial scales such as electron inertial length, Larmor radius and global reconnection length. Therefore it is easily applicable to different space or laboratory plasma situations.

#### Acknowledgments

Author would like to thank Prof. M. Yamada and his team at MRX Princeton Plasma Physics Laboratory for kindly providing their experimental data set and for useful replies to queries. Useful discussions with Dr. G. Vekstein and other participants of Fifts International Cambridge Workshop on Magnetic Reconnection 2008, Bad Honnef, Germany are acknowledged. Author acknowledges useful discussion of solar flare observational aspects with Dr. E. Kontar. Author also would like to thank an anonymous referee who helped to improve the paper significantly. This research was supported by the United Kingdom's Science and Technology Facilities Council (STFC).

- 
- [1] M. Yamada, Y. Ren, H. Ji, J. Breslau, S. Gerhardt, R. Kulsrud, A. Kuritsyn, *Phys. Plasmas* **13**, 052119 (2006).
  - [2] H. Ji, Y. Ren, M. Yamada, S. Dorfman, W. Daughton, and S. P. Gerhardt, *Geophys. Res. Lett.* **35**, 13106 (2008).
  - [3] E. Priest and T. Forbes, *Magnetic reconnection: MHD theory and applications* (Cambridge University Press, 2000).
  - [4] D. Biskamp, *Magnetic reconnection in Plasmas* (Cambridge University Press, 2005).
  - [5] J. Birn and E. R. Priest, *Reconnection of magnetic fields: magnetohydrodynamics and collisionless theory and observations* (Cambridge University Press, 2007).
  - [6] D. E. Innes, B. Inhester, W. I. Axford, *Nature* **386**, 811 (1997).
  - [7] T. N. Woods, *Adv. Sp. Res.* **42**, 895 (2008).
  - [8] J. H. M. M. Schmitt, F. Reale, C. Liefke, U. Wolter, B. Fuhrmeister, A. Reiniers, and G. Peres, *Astron. Astrophys.* **481**, 799 (2008).
  - [9] P. A. Cassak, D. J. Mullan, and M. A. Shay, *Astrophys. J.* **676**, L69 (2008).
  - [10] A. Runov, W. Baumjohann, R. Nakamura, V. A. Sergeev, O. Amm, H. Frey, I. Alexeev, A. N. Fazakerley, C. J. Owen, E. Lucek, *J. Geophys. Res.* **113**, 7 (2008).
  - [11] P. A. Sweet, *Nuovo Cim. Suppl.* **8**, 188 (1958).
  - [12] E. N. Parker, *Astrophys. J. Suppl. Ser.* **8**, 177 (1963).
  - [13] H. E. Petschek, in *In AAS/NASA Symposium on the Physics of Solar Flares*, edited by W. N. Hess (NASA Press, Washington, DC, 1964), pp. 425–437.
  - [14] M. Hesse, K. Schindler, J. Birn, and M. Kuznetsova, *Phys. Plasmas* **6**, 1781 (1999).
  - [15] J. Birn, J. F. Drake, M. A. Shay, B. N. Rogers, R. E. Denton, M. Hesse, M. Kuznetsova, Z. W. Ma, A. Bhattacharjee, A. Otto, *J. Geophys. Res.* **106**, 3715 (2001).
  - [16] P. L. Pritchett, *J. Geophys. Res.* **106**, 3783 (2001).
  - [17] D. Tsiklauri and T. Haruki, *Phys. Plasmas* **14**, 112905 (2007).
  - [18] D. Tsiklauri and T. Haruki, *Physics of collisionless reconnection in a stressed X-point collapse*, *Phys. Plasmas*

- (accepted, inpress) (2008).
- [19] M. M. Kuznetsova, M. Hesse, and D. Winske, *J. Geophys. Res.* **103**, 199 (1998).
  - [20] J. Birn and M. Hesse, *Phys. Plasmas* **14**, 082306 (2007).
  - [21] A. Klimas, M. Hesse, and S. Zenitani, *Phys. Plasmas* **15**, 082102 (2008).
  - [22] G. E. Vekstein and E. R. Priest, *Phys. Plasmas* **2**, 3169 (1995).
  - [23] L. Golub and J. M. Pasachoff, *The Solar Corona* (Cambridge University Press, UK, 1997).
  - [24] R. Horiuchi and T. Sato, *Phys. Plasmas* **4**, 277 (1997).
  - [25] J. A. Breslau and S. C. Jardin, *Phys. Plasmas* **10**, 1291 (2003).
  - [26] M. J. Aschwanden, *Physics of the Solar Corona an Introduction* (Paxis Publishing Ltd, Chichester, UK, 2006).
  - [27] M. Temmer, A. Veronig, A. Hanslmeier, W. Otruba and M. Messerotti, *Astron. Astrophys.* **375**, 1049 (2001).
  - [28] A. Veronig, M. Temmer, A. Hanslmeier, W. Otruba and M. Messerotti, *Astron. Astrophys.* **382**, 1070 (2002).
  - [29] K. Nagashima and T. Yokoyama, *Astrophys. J.* **647**, 654 (2006).
  - [30] W. Daughton, J. Scudder, and H. Karimabadi, *Phys. Plasmas* **13**, 072101 (2006).
  - [31] M. A. Shay, J. F. Drake, and M. Swisdak, *Phys. Rev. Lett.* **99**, 155002 (2007).